Inorg. Chem. **2006**, *45*, 156–161

Syntheses, Structure, and Bonding of $Rb_{14}(Mg_{1-x}In_x)_{30}$. A Nonstoichiometric Phase with an Unusual Substitution in the Anion Framework

Bin Li and John D. Corbett*

Ames Laboratory-DOE[1] and Department of Chemistry, Iowa State University, Ames, Iowa 50011

Received August 22, 2005

The title compound $Rb_{14}(Mg_{1-x}In_x)_{30}$ ($x = 0.79$–0.88) has been obtained from high-temperature reactions of the elements in welded Ta tubes. There is no analogous binary compound without Mg. The crystal structure established by single-crystal X-ray diffraction means (space group $P\bar{6}2m$ (No. 189), $Z = 1$ and $a = b = 10.1593(3)$ Å, $c = 17.783(1)$ Å for $x = 0.851$) features two distinct types of anionic layers: isolated pentacapped trigonal prismatic In_{11}^{7-} clusters and condensed $[(Mg_xIn_{1-x})_5In_{14}]^{7-}$ layers. The latter consists of analogous M_{11} (M = Mg/In) fragments that share prismatic edges and are interbridged by trigonal M_3 units. The structure shows substantial differences from related $A_{15}Tl_{27}$ (A = Rb, Cs) in which the cation A that centers a six-membered ring of Tl_{11} fragments is replaced by M_3. Both linear muffin-tin orbital and extended Hückel calculations are used to analyze the observed phase width and site preferences. We further utilize the results to rationalize the distortion of the M_{11} fragment in the condensed layer and also to correlate with electrical properties. An isomorphous phase region $(Rb_yK_{1-y})_{14}(Mg_{1-x}In_x)_{30}$ ($y = 0.52$, 0.66 for $x = 0.79$) is also formed.

Introduction

The alkali-metal−group 13 (triel) systems are well known for their remarkable structural diversities and novel chemical bonding.[2] Use of mixed alkali metals of different sizes has proven to be very effective in opening routes to new clusters, evidently because two cations of different sizes allow more packing flexibility. A considerable number of novel alkali-metal−indium and −thallium compounds not known in binary systems can be isolated via the size tuning with mixed cations, for example, $Na_2K_{19}Tl_{21}$,[3] $K_3Na_{26}In_{48}$,[4] $Na_4K_6Tl_{13}$,[5] KSr_2In_7,[6] and KNa_3In_9.[7] Another successful means to gain more alkali-metal−triel compounds in exploratory synthesis is to introduce a third element, such as a late transition element, to form ternary or quaternary phases. The capability to tune both size and electron count by this method has led to many new structures with unanticipated clusters. Examples include heterometal-centered clusters of indium and thallium: $Tl_{10}Zn^{8-}$,[8] $In_{10}M^{10-}$ (M = Ni, Pd, Pt),[9] $Tl_{12}M^{12-}$ (M = Mg, Zn, Cd, Hg),[10] and some new clusters, generally large or condensed, such as $Tl_9Au_2^{9-}$,[11] $Tl_8Cd_3^{10-}$,[12] $Tl_{11}Cd_2^{5-}$ chains,[13] $Tl_{10}Cd_9^{7-}$ layers,[14] $(In/Cd)_{18}$ and $(Ga/Ag)_{18}$ tubular clusters,[15] M_{60} buckyballs (M = Al/Zn or Tl/Cd),[16] and triply fused icosahedra $(In/T)_{28}$ (T = Li, Mg, Zn, Au).[17] Often, only modest amounts of the third element are necessary to form structures that are not known in binary systems.

* To whom correspondence should be addressed. E-mail: jcorbett@iastate.edu.

(1) This research was supported by the Office of the Basic Energy Sciences, Materials Sciences Division, U. S. Department of Energy (DOE). The Ames Laboratory is operated for DOE by Iowa State University under Contract No. W-7405-Eng-82.

(2) Corbett, J. D. In *Chemistry, Structure and Bonding of Zintl Phases and Ions*; Kauzlarich S., Ed.; VCH Publishers: New York, 1996; Chapter 3. Corbett, J. D. *Angew. Chem., Int. Ed.* **2000**, *39*, 670. Belin, C. H. E.; Charbonnel, M. *Prog. Solid State Chem.* **1993**, *22*, 59.
(3) Dong, Z.-C.; Corbett, J. D. *J. Am. Chem. Soc.* **1994**, *116*, 3429.
(4) Sevov, S. C.; Corbett, J. D. *Inorg. Chem.* **1993**, *23*, 1612.
(5) Dong, Z.-C.; Corbett, J. D. *J. Am. Chem. Soc.* **1995**, *117*, 6447.
(6) Chi, L.-S.; Corbett, J. D. *Inorg. Chem.* **2001**, *40*, 3596.
(7) Li, B.; Corbett, J. D. *Inorg. Chem.* **2002**, *41*, 3944.
(8) Dong, Z.-C.; Henning, R. W.; Corbett, J. D. *Inorg. Chem.* **1997**, *36*, 3559.
(9) Sevov, S. C.; Corbett, J. D. *J. Am. Chem. Soc.* **1993**, *15*, 9089.
(10) Dong, Z.-C.; Corbett, J. D. *Angew. Chem., Int. Ed. Engl.* **1996**, *35*, 1006.
(11) Dong, Z.-C.; Corbett, J. D. *Inorg. Chem.* **1995**, *34*, 5042.
(12) Huang, D.-P.; Corbett, J. D. *Inorg. Chem.* **1999**, *38*, 316.
(13) Kaskel, S.; Corbett, J. D. *Inorg. Chem.* **2000**, *39*, 3086.
(14) Tillard-Charbonnel, M.; Chahine, A.; Belin, C.; Rousseau, R.; Canadell, E. *Chem.−Eur. J.* **1997**, *3*, 799.
(15) Flot, D. M.; Tillard-Charbonnel M.; Belin, C. H. E. *J. Am. Chem. Soc.* **1996**, *118*, 5229. Henning, R. W.; Corbett, J. D. *Z. Anorg. Allg. Chem.* **2002**, *628*, 2715.
(16) Lee, C.-S.; Miller, G. J. *J. Am. Chem Soc.* **2000**, *122*, 4937. Lee, C.-S.; Miller, G. *Inorg. Chem.* **2001**, *40*, 338. Li, B.; Corbett, J. D. *Inorg. Chem.* **2004**, *43*, 3582.
(17) Li, B.; Corbett, J. D. *J. Am. Chem. Soc.* **2005**, *127*, 926. Li, B.; Corbett, J. D. unpublished research.

10.1021/ic0514290 CCC: $33.50
Published on Web 11/19/2005

Ongoing research on such systems continues to show that derivatization of a triel cluster phase by the third element is a promising route to synthesize compounds with new structures. The $A_{15}Tl_{27}$ (A = Rb, Cs)[18] structure discovered in our group around a decade ago shows not only unusual structural features in the presence of different Tl_{11} skeletons but also possible means for electronic tuning. According to semiempirical tight-binding band calculations, these compounds should be tuned into Zintl phases if two electrons per formula were either added to or subtracted from the layers. However, attempts to tune such to a Zintl phase by doping with a third element have not yet succeeded.[18] In view of the similarities found for thallium vs indium clusters, for example, Tl_{11}^{7-} and In_{11}^{7-} found in A_8Tl_{11} (A = K, Rb, Cs)[19] and A_8In_{11} (A = K, Rb),[20] respectively, we looked into A−In systems for an isotype of $A_{15}Tl_{27}$. Not surprisingly, none was found in the binary Rb−In system, perhaps because the stable Rb_2In_3[21] (60% In) is close to that sought, $Rb_{15}In_{27}$ (64.3% In). However, introduction of a modest amount of magnesium leads to the first (quasi-)ternary Rb−Mg−In compound with a structure that is closely related to that of $Rb_{15}Tl_{27}$. We report here the syntheses, structural characterizations, and the electronic structure of and chemical bonding within this new phase region.

Experimental Section

Syntheses. All materials were handled in N_2-filled gloveboxes with moisture levels below 1 ppm (vol). All three compounds were synthesized via high-temperature reactions of the elements (99.95% rubidium chunks, 99.95% potassium chunks, 99.99% magnesium, and 99.999% indium tear drops, all from Alfa-Aesar). The weighed elements were enclosed in welded tantalum tubes that were in turn sealed in evacuated fused silica jackets by methods and techniques described previously.[22]

Several single crystals of $Rb_{14}(Mg_{1-x}In_x)_{30}$ ($x = 0.876$) (**1**) were first obtained from the In-richer $Rb_{13}Mg_2In_{27}$ and $Rb_{15}Mg_2In_{25}$ compositions during attempts to gain compounds with closed shells that are isostructural with $A_{15}Tl_{27}$.[18] However, structure refinements showed a new structure with a substantial and interesting difference in which one A cation site in $A_{15}Tl_{27}$ had been replaced by a trigonal $(In/Mg)_3$ unit. Two of seven anionic sites refined as co-occupied by Mg and In, but there was no independent Mg site. As expected, a phase width was found in the two refined single-crystal compositions $Rb_{14}(Mg_{1-x}In_x)_{30}$, $x = 0.851$ (**2**) and $x = 0.792$ (**3**) obtained from loaded compositions $Rb_{14}Mg_{4.5}In_{25.5}$, $x = 0.85$, and $Rb_{14}Mg_9In_{21}$, $x = 0.70$, respectively. Products from two later reactions with $Rb_{14}Mg_3In_{27}$ and $Rb_{14}Mg_9In_{21}$ compositions had the same lattice constants for each main phase as those refined from single crystals **1** and **3** plus ∼7% Rb_2In_3 and ∼10% unknown phases, respectively. This confirmed a phase width x of 0.79 (**3**) to 0.88 (**1**) at 250 °C.

The tolerance for different-sized cations in the related structure of $A_{15}Tl_{27}$ (A = Rb, Cs) also led us to attempt to substitute Cs or K for Rb in the present work, but only a portion of the Rb could be replaced by K and none by Cs. Two single crystals of $(Rb_yK_{1-y})_{14}(Mg_{1-x}In_x)_{30}$ refined as $y = 0.52$, $x = 0.79$ (**4**) and $y = 0.66$, $x = 0.79$ (**5**) showed that both are isostructural with title structure type and that all three alkali metal sites are co-occupied by K and Rb (see Supporting Information). Once the stoichiometries of all five compounds had been established by crystallography, the pure phases were synthesized directly from the appropriate compositions (judging from comparisons of their Guinier powder patterns with those calculated from the refined structures). All are made by heating the samples at 500 °C for 10 h, then cooling at 3 °C/h to 250 °C, and holding them there for 160 h to grow crystals. All five are silvery, brittle, and very sensitive to moisture and air. Although there is no independent Mg crystallographic position, attempts to synthesize the isostructural but binary Rb−In compound failed. The third element, Mg, is necessary to stabilize this structure.

X-Ray Studies. X-ray diffraction investigations were performed on powdered and single crystals. Powder diffraction data were collected with the aid of a Huber 670 Guinier powder camera equipped with an area detector and Cu K_α radiation ($\lambda = 1.540598$ Å). Peak search, indexing, and least-squares refinements for cell parameters were done with the WinXPOW program.[23] Diffraction data from **2**, **4**, and **5** were collected at 293 K on a Bruker SMART APEX CCD diffractometer with Mo K_α radiation and were harvested from three sets of 606 frames with 0.3° scans in ω and exposure times of 10 s per frame. The 2θ range extended from ∼3° to ∼57°. The unit cell parameters for each were determined from data for about 900 indexed reflections. The reflection intensities were integrated with the SAINT subprogram in the SMART software package.[24] The data were corrected for Lorentz and polarization effects, and the program SADABS[25] was applied for empirical absorption corrections. Diffraction data from **1** and **3** were collected at 293 K on a STOE IPDS II single-crystal X-ray diffractometer with Mo K_α radiation using the supplied STOE software.[26] The data were corrected for Lorentz and polarization effects, and a numerical absorption correction was accomplished with the program X-SHAPE.

All the structure solutions were obtained by direct methods and refined by full-matrix least-squares refinement of F_o^2 using the Bruker SHELXTL 6.1 software package.[27] The data sets show no systematic absences, and intensity statistics gave a clear indications of non-centrosymmetric space groups (for example, $|E^2 - 1| = 0.777$ for **2**). The assignments of the extinction-free space group $P\bar{6}2m$ (No. 189) were also supported by the subsequent successful refinements. For **2**, direct methods provided nine peaks, of which six were assigned to In and three to Rb atoms according to distances and peak heights. A few least-squares cycles followed by a difference Fourier map revealed one less strongly diffracting atom with distances appropriate for indium, and it was so assigned. However, it became clear after a few more cycles that indium alone was too strong a scatterer at the In4 and In7 positions. At this point, R1 and the highest difference peak were 0.088 and 7.9 e/Å^3, respectively. Allowing mixtures of magnesium and indium at the two positions with varying isotropic displacement parameters gave significant improvements in R1 (0.059) and the highest difference

(18) Dong, Z.-C.; Corbett, J. D. *Inorg. Chem.* **1996**, *35*, 1444.
(19) Dong, Z.-C.; Corbett, J. D. *J. Cluster Sci.* **1995**, *6*, 187.
(20) (a) Sevov, S. C.; Corbett, J. D. *Inorg. Chem.* **1991**, *30*, 4875. (b) Blase, W.; Cordier, G.; Somer, M. *Z. Kristallogr*. **1991**, *194*, 150. (c) Blase, W.; Cordier, G.; Müller, V.; Häussermann, U.; Nesper, R. *Z. Naturforsch. B* **1993**, *48*, 754. (d) Cordier, G.; Müller, V. *Z. Kristallogr*. **1993**, *203*, 154.
(21) Sevov, S. C.; Corbett, J. D. *Z. Anorg. Allg. Chem.* **1993**, *619*, 128.
(22) Dong, Z.-C.; Corbett, J. D. *J. Am. Chem. Soc*. **1993**, *115*, 11299.
(23) *STOE WinXPOW 2.10*; STOE and Cie GmbH: Hilpertstr, Darmstadt, Germany, 2004.
(24) *SMART*; Bruker AXS, Inc.; Madison, WI, 1996.
(25) Blessing, R. H. *Acta Crystallogr*. **1995**, *A51*, 33.
(26) (a) *IPDS II*; Stoe and Cie Gmbh: Darmstadt, Germany, 2002. (b) *XSHAPE, revision 2.03: Crystal Optimization for Numerical Absorption Correction*; Stoe and Cie Gmbh: Darmstadt, Germany, 2003.
(27) *SHELXTL*; Bruker AXS, Inc.; Madison, WI, 2000.

Table 1. Single-Crystal Data and Structure Refinements for $Rb_{14}(Mg_{1-x}In_x)_{30}$ with $x = 0.876$ (**1**), 0.851 (**2**), 0.792 (**3**), and $(Rb_yK_{1-y})_{14}(Mg_{1-x}In_x)_{30}$ ($x = 0.787$) for $y = 0.52$ (**4**) and 0.66 (**5**)

compounds	**1**	**2**	**3**	**4**	**5**
fw	4304.48	4238.41	4073.68	3747.06	3842.10
space group, Z	$P\bar{6}2m$, 1	$P\bar{6}2m$, 1	$P\bar{6}2m$, 1	$P\bar{6}2m$, 1	$P\bar{6}2m$, 1
a (Å)[a]	10.188(1)	10.1593(3)	10.065(1)	10.010(1)	10.0288(3)
c (Å)	17.798(4)	17.789(1)	17.947(4)	17.592(4)	17.7005(9)
vol (Å^3)	1599.9(4)	1589.5(1)	1574.6(4)	1526.5(4)	1541.8(1)
ρ_{calc} (g/cm^3)	4.467	4.428	4.296	4.076	4.138
μ(Mo Kα) (mm^{-1})	19.874	19.754	19.308	14.956	16.266
R1/wR2, $I > 2\sigma(I)$ (%)	3.64/5.91	2.66/6.19	2.82/5.37	1.97/ 4.07	1.90/3.80
R1/wR2, all data (%)	5.16/6.12	2.94/7.67	3.34/5.51	2.10/4.19	2.12/3.95
largest diff. peak and hole (e·Å^{-3})	0.869, −0.915	1.10, −0.69	1.57, −1.06	1.05, −0.578	0.62, −0.477

[a] Diffractometer refinements

Table 2. Atomic Coordinates and Isotropic-Equivalent Displacement Parameters (Å$^2 \times 10^3$) for **2**

atom	site	x	y	z	U(eq)[b]
In1	2e	0	0	0.1405(1)	26(1)
In2	3f	0.7909(1)	0	0	25(1)
In3	6i	0.2794(1)	0	0.0873(1)	31(1)
M4[a]	6k	0.1724(2)	0.4768(2)	1/2	22(1)
In5	6i	0.5928(1)	0	0.3999(1)	27(1)
In6	4h	1/3	2/3	0.3485(1)	26(1)
M7[a]	3g	0.8288(2)	0	1/2	30(1)
Rb1	6i	0.6046(2)	0	0.1873(1)	44(1)
Rb2	2c	2/3	1/3	0	47(1)
Rb3	6i	0.2518(1)	0	0.3154(1)	33(1)

[a] The M4 and M7 sites are fully occupied by Mg and In mixtures (details in Table 4). [b] U(eq) is defined as one-third of the trace of the orthogonalized U_{ij} tensor.

Table 3. Selected Bond Distances (Å) in $Rb_{14}(Mg_{1-x}In_x)_{30}$: $x = 0.876$ (**1**), 0.851 (**2**), and 0.792 (**3**) and the Corresponding −ICOHP (eV) Per Bond According to a $Rb_{14}Mg_5In_{25}$ Model, $x = 0.833$

bond	**1**	**2**	**3**	−ICOHP
In1−In2	3.290(2)	3.280(1)	3.282(1)	0.83
In1−In3	3.001(1)	2.992(1)	2.986(1)	1.58
In2−In3	2.997(1)	2.9920(8)	2.9899(9)	1.41
In3−In3	3.109(3)	3.105(1)	3.107(2)	1.06
M4−M4[a]	3.026(5)	3.034(3)	3.057(7)	1.10
M4−M4[a]	3.138(5)	3.118(3)	3.062(6)	0.75
M4−In5	3.117(3)	3.113(1)	3.106(3)	0.64
M4−In5	3.338(2)	3.323(1)	3.281(3)	0.42
M4−In6	3.251(2)	3.240(1)	3.242(2)	0.75
M4−M7	3.107(3)	3.098(2)	3.070(4)	1.16
In5−In5	3.569(3)	3.560(1)	3.556(1)	0.34
In5−In6	3.2221(8)	3.2134(5)	3.1917(7)	1.17
In5−M7	2.993(2)	2.986(1)	2.984(1)	1.16
M7−M7	3.023(4)	3.013(3)	2.960(3)	1.56

[a] The shorter M4−M4 corresponds to intercluster bonding, and the longer to intracluster interactions.

peak (4.95 e/Å^3, 0.51 Å from Rb1), whereas occupancy refinements of the assigned In1,2,3,5,6 sites all fell in the region of 100(2)% In. Refinements, finally with anisotropic displacement parameters and a secondary extinction correction, converged at R1 = 0.027, wR2 = 0.062 ($I > 2\sigma(I)$). No peak (>0.5 e/Å^3) was found at the 1*b* site occupied by Rb4 in $Rb_{15}Tl_{27}$.

The single-crystal structures for the other four compounds were similarly solved and refined. The details of the crystallographic and refinement parameters for all five compounds are given in Table 1. Because of the isostructural character of the five compounds, Table 2 only gives the corresponding atomic positional and isotropic-equivalent displacement parameters for **2** as an example. Table 3 contains the important interatom distances for the three Rb−In−Mg compounds (**1**, **2**, **3**), and their refined site occupancies are given in Table 4. More detailed crystallographic and refinement

Table 4. Experimental Site Occupancies in **1**, **2**, and **3**, and Total Mulliken Populations (MP) and Valence s Orbital Populations (MPs) for Each Atom Site, from EHTB Calculations on an In_{30}^{-14} Model

atom		site occ. in different compounds				
		1	**2**	**3**	MP	MPs
In1		1	1	1	3.53	1.38
In2		1	1	1	3.32	1.33
In3		1	1	1	3.83	1.49
M4	In	0.444(8)	0.356(5)	0.117(6)	2.57	1.19
	Mg	0.556	0.644	0.883		
In5		1	1	1	3.03	1.28
In6		1	1	1	3.61	1.43
M7	In	0.87(1)	0.803(8)	0.687(9)	3.28	1.20
	Mg	0.13	0.197	0.313		

data and the anisotropic displacement parameters for all compounds are available in the Supporting Information (cif).

Physical Property Measurements. Electrical resistivities were measured by the electrodeless "Q" method with the aid of a Hewlett-Packard 4342A Q meter.[28] The method is particularly suitable for measurements on highly air-sensitive samples. For this purpose, 48.5 mg of powdered $Rb_{14}(Mg_{1-x}In_x)_{30}$ ($x = 0.851$) (**2**) with grain diameters between 150 and 250 μm was dispersed with chromatographic alumina and sealed into Pyrex tubes. Measurements were made at 34 MHz over the range 80−260 K. The measured resistivities increase linearly over the range, which is taken as the defining characteristic of a metal. The extrapolated ρ_{298} value is about 65.2 $\mu\Omega$·cm. Magnetic susceptibility data for this compound were obtained from a 49.0 mg ground powder sealed under He in the container type described elsewhere.[29] The magnetization was measured over the range 6−350 K on a Quantum Design MPMS SQUID magnetometer. The results show almost temperature-independent paramagnetism, $\sim 2.5 \times 10^{-3}$ emu/mol, over 50−330 K after corrections for the container and the diamagnetic cores of the atoms. Graphical data of the electrical resistivities and magnetic susceptibilities are in the Supporting Information.

Electronic Structure Calculations. Electronic structure calculations were performed with both tight-binding linear muffin-tin orbital (TB-LMTO-ASA) and extended Hückel (EHTB) methods in order to assess chemical bonding in the structure, to understand the phase width, and to rationalize the preferential occurrence of substitution defects in the clusters. To reflect the mixed Mg/In site occupancies of the M4 and M7 sites, LMTO calculations were carried out in subgroup *Amm*2 (No.38) in the atomic sphere approximation using the LMTO47 program.[30] On descent from

(28) Zhao, J. T.; Corbett, J. D. *Inorg. Chem.* **1995**, *34*, 378.
(29) Sevov, S. C.; Corbett, J. D. *Inorg. Chem.* **1991**, *30*, 4875.
(30) van Schilfgarde, M.; Paxton, T. A.; Jepsen, O.; Andersen, O. K.; Krier, G. In *Program TB-LMTO*; Max-Plank-Institut fur Festkorperforschung: Stuttgart, Germany, 1994.

$P\bar{6}2m$ to $Amm2$ ($a' = b$, $b' = 2\vec{a} + \vec{b}$, $c' = b$), the cell doubles, the M4 site (6*k*) splits into three 4*e* sites, and the M7 site (3*g*) to one 2*b* and one 4*e* site. According to the observed occupancies at M4 and M7 sites (Table 4), two of the three 4*e* sites and the 2*b* site were assigned as Mg and the remainder as In. These assignments not only roughly reflect the relative occupancies of each original site but also correspond to $Rb_{14}Mg_5In_{25}$ composition, right in the middle of the observed phase width. Different distributions of Mg into the three 4*e* sites did not generate any meaningful differences in terms of total energy, as well as in our calculational results. The radii of the Wigner−Seitz (WS) spheres were assigned automatically so that the overlapping potential would be the best possible approximation to the full potential.[31] No interstitial sphere was necessary with the default overlap restriction (16%). The WS radii determined by this procedure for the atoms were 3.24−3.48 Å for In, 3.12−3.35 Å for Mg, and 4.52−5.40 Å for Rb.

Semiempirical EHTB band calculations[32] were carried out on a hypothetical cluster ion $[In_{30}]^{14-}$ to study the "coloring problem", i.e., the site preferences for Mg vs In throughout the anionic clusters. EHTB calculations are useful here because they allow a Mulliken atom population analysis, which provides insight into charge segregation within the anionic framework.[16] The valence orbitals of the Rb atoms were excluded from these calculations, but their valence electrons were utilized. Mulliken populations for valence orbital occupations were evaluated by integrating over a set of 396 **k**-points in the irreducible wedge of the primitive hexagonal Brillouin zone. Atomic orbital parameters used for indium are: $H_{ii}(5s) = -12.6$, $H_{ii}(5p) = -6.19$, $\xi(5s) = 1.903$, and ξ (5p) = 1.677 (H_{ii} = orbital energy, eV; ξ = Slater exponent).[33]

Results and Discussion

Crystal Structures. All five compounds are isotypic and feature a new structure type in which layers of isolated In_{11}^{7-} clusters (D_{3h}) alternate with condensed two-dimensional layers $^2_\infty[M_5In_{14}^{7-}]$ (M = In/Mg), Figure 1. The neighboring cluster layers are separated by double rubidium layers of Rb1 and Rb3 atoms, whereas Rb2 lies within the layer of separate In_{11}^{7-} clusters. The shortest distance between alkali-metal atoms is the ∼4.2 Å Rb1−Rb2 separation. The closest interlayer In−In separation is ∼6.19 Å, between atoms in the adjacent layers, In1 and In5. Such isolated In_{11}^{7-} clusters with D_3 point group symmetry are known in A_8In_{11} (A = K, Rb) compounds.[20] As shown in Figure 2a, the In−In separations range from 2.992(1) to 3.280(1) Å with a 3.071 Å average over the polyhedron, substantially the same as the ∼3.070 Å average in K_8In_{11}[20a] and 3.069 Å in $Rb_8In_{11}Cl$ (the reported Rb_8In_{11} cannot be reproduced).[34] The unusual feature of this structure is the condensed layer formed by similar M_3In_8 fragments that share the three prismatic edges (In5−In5) and are interbridged via $(M7)_3$ trigonal units that center six-membered rings of M_3In_8 (Figure 3a). In comparison with the isolated In_{11} (D_{3h}) clusters, the M_3In_8 (C_{3h}) fragments (Figure 2b) in the layer are altered by the condensation, the waist-capping atoms moving significantly toward the rectangular prism faces, decreasing their separations from 3.68 (In2−In2 in In_{11}) to 3.12 Å (In4−In4 in M_3In_8). Correspondingly, the prism heights increase from 3.11 to 3.56 Å, the axial lengths, from 5.00 to 5.39 Å, and the basal plane edges of the prisms, from 4.92 to 5.34 Å.

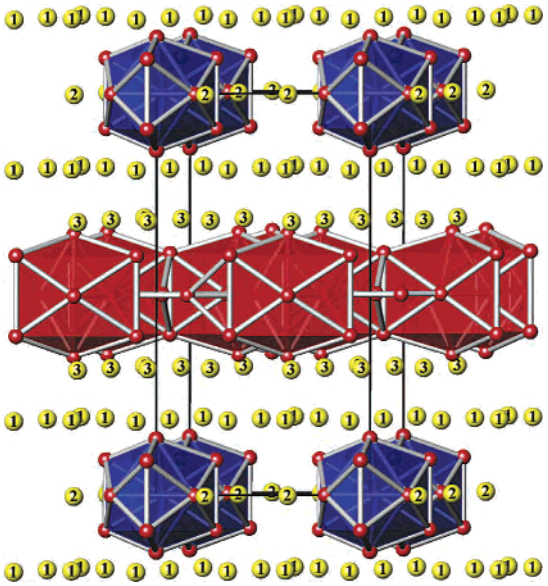

Figure 1. ∼[100] view of the unit cell of $Rb_{14}(Mg_{1-x}In_x)_{30}$ with layers of cations (yellow), isolated In_{11} (blue), and condensed M_{19} (red) clusters (M = Mg/In). *c* lies vertically.

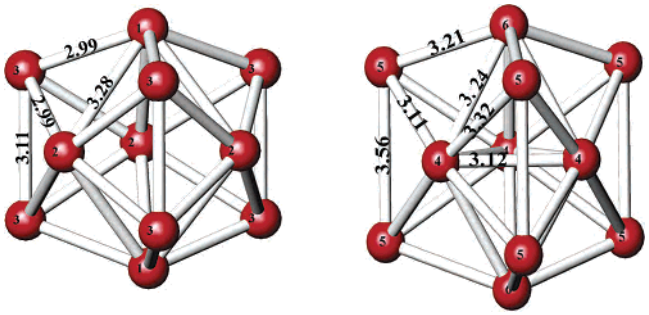

Figure 2. $Rb_{14}(Mg_{1-x}In_x)_{30}$: (a) isolated In_{11}^{7-} polyanions (D_{3h}); (b) M_3In_8 cluster fragment (C_{3h}) in the condensed layer. The bond distances are for compound **2**.

On the other hand, the dimensions of this fragment also vary with Mg content, which is reasonable considering the different metallic radii of Mg (1.36 Å) and In (1.44 Å).[35] Presumably, the condensed layer will not be stable when alterations of its dimensions become too large, which may account for the narrow phase width. As shown in Table 3, the M4−M4 intracluster distances decrease from 3.14 to 3.06 Å from **1** to **3**, and the same intercluster distances increase from 3.03 to 3.06 Å. It is interesting to note that this adverse distance change limits the Mg content at the M4 site and thus the upper limit of Mg in this part of the phase in order to optimize both bonds at the same time. The prism height (In5−In5) and the axial separation (In6−In6) also change with inward movement of the M4 atoms, increasing the axial length (In6−In6) from 5.39 to 5.44 Å between **1** and **3**, the phase limits. This nicely explains the unusual increase of the *c* axis over the phase width in parallel with the Mg

(31) Jepsen, O.; Andersen, O. K. *Z. Phys. B* **1995**, *97*, 35.
(32) Ren, J.; Liang, W.; Whangbo, M.-H. *CAESAR for Windows*: Prime-Color Software, Inc., North Carolina State University: Raleigh, NC, 1998.
(33) Canadell, E.; Eisenstein, O.; Rubio, J. *Organometallics* **1984**, *3*, 759.
(34) Henning, R. W.; Corbett, J. D. *Inorg. Chem.* **1997**, *36*, 6045.
(35) Pauling, L. *Nature of the Chemical Bond*, 3rd ed.; Cornell University, Press: Ithaca, NY, 1960; p 403.

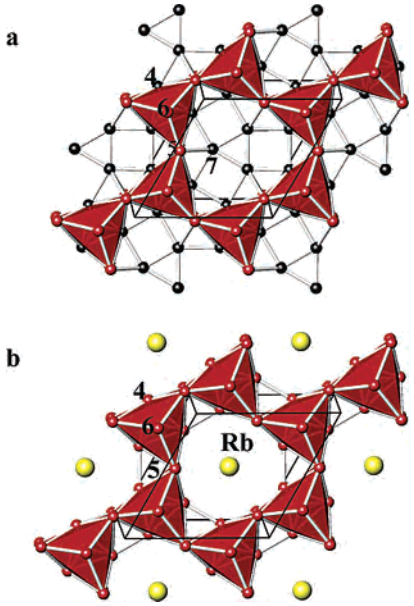

Figure 3. [001] projections of the condensed layers with (a) a $(M7)_3$ trigonal centering unit in $Rb_{14}(Mg_{1-x}In_x)_{30}$ and (b) a single Rb4 atom that centers the network layer in $Rb_{15}Tl_{27}$. The mixed In/Mg sites are black in the former.

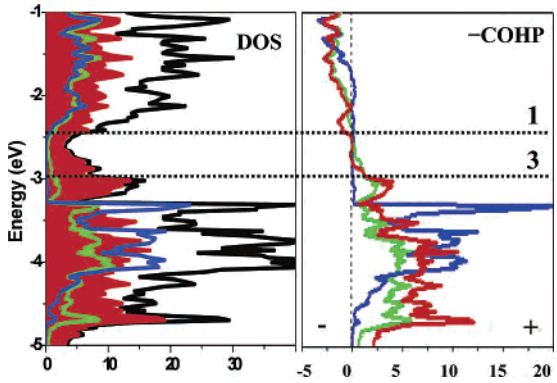

Figure 4. TB-LMTO-ASA electronic structure calculation results for $Rb_{14}Mg_5In_{25}$. Left: total DOS (black) and partial DOS curves for rubidium (green line), isolated In_{11} cluster (blue line), and condensed layer $[Mg_5In_{14}]$ (red shaded region). Right: −COHP curves for three different interactions: In−In within isolated In_{11} clusters (blue line), M−M within M_{11} fragment (green line), and M−M within the condensed Mg_5In_{14} layer (red line). The two dotted lines denote the Fermi levels for **1** (upper) and **3** (lower).

increase, whereas *a* and the volume decrease. Even though there is only a small change of the long edge-shared In5−In5 bond, these distances (3.57 Å in **1**) are larger than those commonly seen in other indium systems with bridged or isolated clusters, 2.85−3.1 Å, the shorter appearing particularly in two-center intercluster links.[7,17,36] This longer bond is correspondingly weaker according to integrated −ICOHP analysis (below). Of course, the stability of the structure does not depend on only one bond interaction, but rather on a complex combination of all bond interactions.

Compared with the $A_{15}Tl_{27}$ structure,[18] this structure is substantially different because of the substitution of a trigonal $(M7)_3$ unit in the condensed layers in place of a single Rb or Cs atom in the former (Figure 3). This seems to be rare in intermetallic systems. This centering $(M7)_3$ unit is also bonded to In5 and M4 atoms with distances that seem to be normal. However, the distances from the center of the six-cluster ring to the neighboring M4 and In5 atoms are 4.25 and 4.50 Å, respectively, meaning that the cavity is too large for Rb judging from the average Rb−In distance of 3.98 Å in $Rb_8In_{11}Cl$.[20d,34] Another reason for this might be that Rb_2In_3 with a similar composition to $Rb_{15}In_{27}$ appears to be relatively stable, in contrast to other A_2In_3 members.[34]

Electronic Structure and Chemical Bonding. Figure 4 displays the densities-of-states (DOS) and crystal orbital Hamilton population (−COHP) analyses of $Rb_{14}Mg_5In_{25}$ on the basis of TB-LMTO-ASA theory. The left part shows the total DOS (black) and projections for isolated In_{11} cluster (blue), the condensed Mg_5In_{14} layer (red), and the rubidium atoms (green), and the COHP results (right) describe bonding in the isolated cluster (blue), in the hypothetical M_3In_8 fragments (green) and in the Mg_5In_{14} condensed layers (red). The two dashed lines correspond to Fermi levels at the phase boundaries of **1** (−2.42 eV) and **3** (−2.91 eV) with 100.3 and 97.8 valence electrons per cell, respectively. Data for the isolated In_{11}^{7-} clusters in both parts of Figure 4 (blue lines) indicate that a closed-shell configuration is achieved below E_F, whereas the condensed layer exhibits major contributions to DOS across the phase width. Rubidium shows some contributions to the overall DOS up to E_F, especially in **1**, and this originates mainly with Rb1 and Rb3 atoms that separate the neighboring cluster layers.

Clearly, the region with low but nonzero total DOS compares fairly well with the observed phase width, and the −COHP curves over this region indicate correspondingly nearly nonbonding interactions. The In−In bonding states within the condensed layer in **3** are not completely filled at the Fermi level, and an increase of valence electron concentration on a decrease of the Mg content strengthens these. The COHP values for all bonds within the M_3In_8 fragment are optimized near the Fermi level of **1** (green). A trace of antibonding at the upper limit comes from interactions within the central trigonal unit $(M7)_3$ and between this and the $(M4)_3In_8$ fragments, i.e., for M7−M7, M7−M4, and M7−In5 (red). The E_F for **2,** a mid-composition, cuts through a finite DOS at −2.56 eV, which is consistent with its poor metallicity according to both resistivity and magnetic susceptibility measurements (Supporting Information).

To provide more details on the different interactions, the pairwise −ICOHP values per bond are also listed in Table 3. These bond strength measures are consistent with interatomic distances in the system. In the condensed layer, all interactions within the central trigonal $(M7)_3$ unit and between this and the M_{11} fragments (M7−M4 and M7−In5) have large −ICOHPs (1.16−1.65 eV/bond), whereas all interactions within the M_3In_8 fragment have small values (0.34−0.75 eV/bond) except for In5−In6. The −ICOHP value for the long In5−In5 bond (0.35 eV) is especially small, as expected. The system successfully satisfies the most

(36) Sevov, S. C.; Corbett, J. D. *Inorg. Chem.* **1992**, *32*, 1895. Sevov, S. C.; Corbett, J. D. *J. Solid State Chem.* **1993**, *103*, 114. Sevov, S. C.; Corbett, J. D. *Inorg. Chem.* **1993**, *32*, 1059. Li, B.; Corbett, J. D. *Inorg. Chem.* **2003**, *42*, 8768.

important chemical interactions by effectively adjusting the Fermi level via the stoichiometry and structure.

To understand the specific substitution of Mg at the M4 and M7 sites, EHTB calculations were also carried out on an anionic network with In parameters for all atoms and 99 valence electrons per unit cell, an intermediate point in phase width. Here it is assumed that the rubidium atoms simply donate their electrons to the anionic lattice of the more electronegative elements. Table 4 summarizes the total Mulliken populations (MP) and those for just the In s orbitals (MPs) for all seven crystallographic sites in the In_{30}^{-14} anion. Among all seven sites, that corresponding to the M4 site has the lowest MP, or the least negative charge, making it the best candidate for Mg substitution, whereas that corresponding to the M7 site with the lowest Mg content (Table 4) is third in low MP. On the other hand, both the M4 and M7 sites have the lowest s- and the largest p-orbital populations. It appears that not only the low total Mulliken populations but also the lower valence s-orbital populations enhance Mg occupation of the M4 and M7 sites. However, site preference energies can of course also bias these population trends,[16] this being reasonable for the M7 position as it has the smallest number of In neighbors.

Conclusions

The first phase in the Rb−Mg−In system, $Rb_{14}(Mg_{1-x}In_x)_{30}$ ($0.79 \leq x \leq 0.88$), has been established, and the structure refined from single-crystal X-ray diffraction data at three compositions. This new structure is closely related to that of $A_{15}Tl_{27}$ (A = Rb, Cs) structure except for substitution of a trigonal $(In/Mg)_3$ group in place of the A cations in the condensed layer in the latter. The discovery of this novel structure once again illustrates how introduction of a third element in alkali-metal−triel systems can be an effective route to new structures. The driving force to optimize the important bonding in the condensed network appears decisive for the formation of this new phase in which heteroatoms are used to alter the electronic requirements.

Acknowledgment. We are indebted to S. Budko for the magnetic susceptibility data.

Supporting Information Available: Refinement parameters for all five compounds in cif format, and figures of resistivity and magnetic susceptibility data. This material is available free of charge via the Internet at http://pubs.acs.org.

IC0514290